How to cite: *Angew. Chem. Int. Ed.* **2021**, *60*, 15214–15219
International Edition: doi.org/10.1002/anie.202101909
German Edition: doi.org/10.1002/ange.202101909

DNA Nanotechnology | Hot Paper

Reversible Supra-Folding of User-Programmed Functional DNA Nanostructures on Fuzzy Cationic Substrates

Koyomi Nakazawa, Farah El Fakih, Vincent Jallet, Caroline Rossi-Gendron, Marina Mariconti, Léa Chocron, Mafumi Hishida, Kazuya Saito, Mathieu Morel, Sergii Rudiuk, and Damien Baigl**

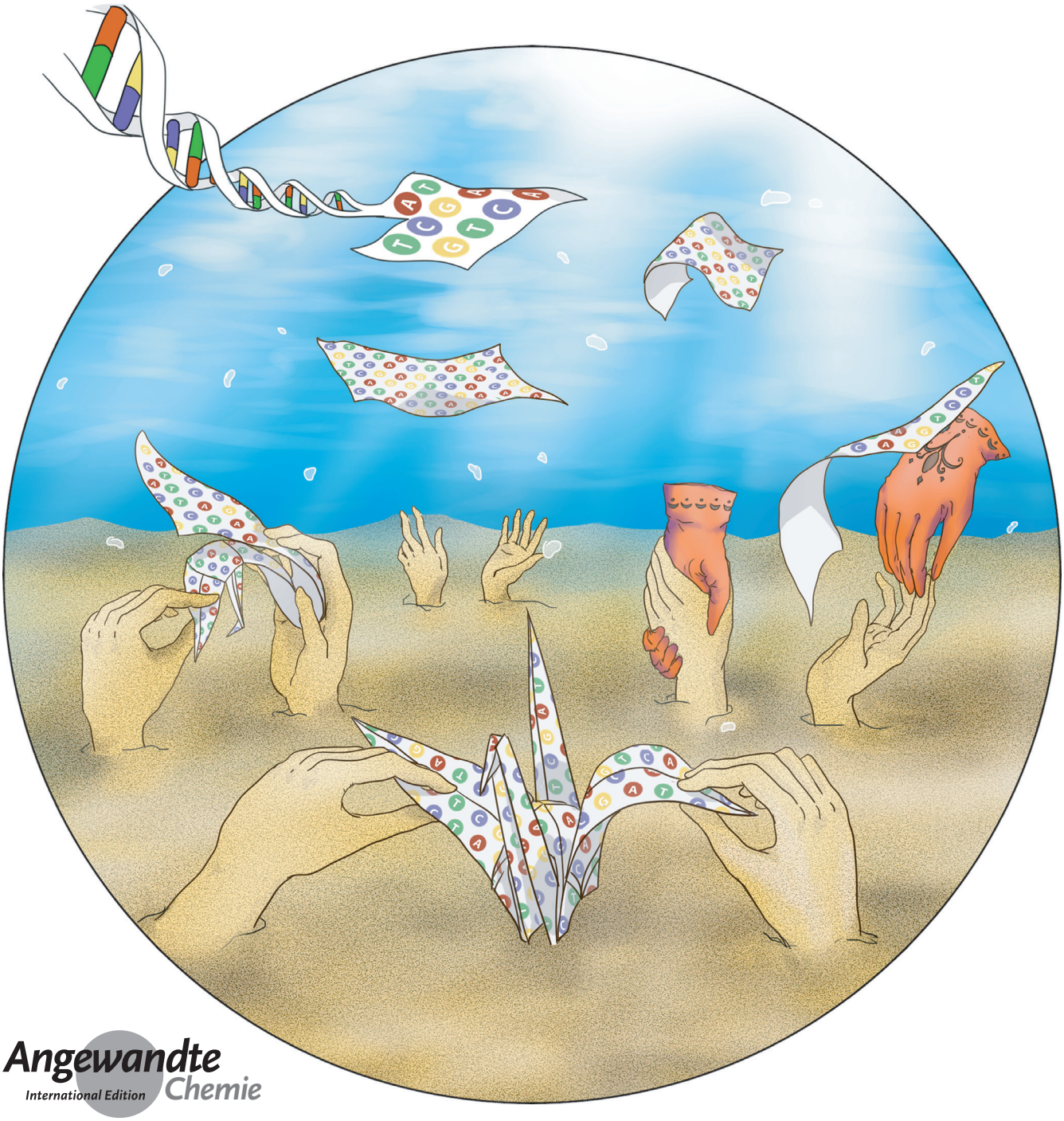

Abstract: *We report that user-defined DNA nanostructures, such as two-dimensional (2D) origamis and nanogrids, undergo a rapid higher-order folding transition, referred to as supra-folding, into three-dimensional (3D) compact structures (origamis) or well-defined μm-long ribbons (nanogrids), when they adsorb on a soft cationic substrate prepared by layer-by-layer deposition of polyelectrolytes. Once supra-folded, origamis can be switched back on the surface into their 2D original shape through addition of heparin, a highly charged anionic polyelectrolyte known as an efficient competitor of DNA-polyelectrolyte complexation. Orthogonal to DNA base-pairing principles, this reversible structural reconfiguration is also versatile; we show in particular that 1) it is compatible with various origami shapes, 2) it perfectly preserves fine structural details as well as site-specific functionality, and 3) it can be applied to dynamically address the spatial distribution of origami-tethered proteins.*

DNA preserves and transfers genetic information owing to the complementarity between two polynucleotide strands assembled according to Watson–Crick base-pairing.[1] The strong specificity of hydrogen bonding within the base-pairs is a unique property of DNA which has enabled wide applications not only in biomedical research but also in materials science, with the development of molecular computers and programmed self-assembly systems.[2–5] One widely used approach consists in folding a long single-stranded circular DNA template chain into intended two-dimensional (2D) nanostructures called DNA origamis, by specific hybridization with a large number of short single-stranded DNA oligonucleotides (staples).[6] This technique enables the realization of DNA nanostructures of virtually any desired shape[7–10] with high site accuracy and yield.[11] To achieve nanosystems with advanced functionalities, efforts have been devoted to increase the structural complexity of DNA origamis, especially to build three-dimensional (3D) nano-objects[8,9,12–15] and/or to render these nanostructures dynamic with the realization of stimulus-responsive behavior or on-demand morphological change capability.[15–17] This was mostly achieved by either exploiting DNA base pairing principles, such as strand-displacement strategies[18] to program dynamic reconfigurability, or modifying DNA to make it stimulus-responsive. To complement these well-established yet sequence- or system-specific approach, it is valuable to look for new actuation approaches which could be orthogonal to DNA base-pairing and without need of DNA covalent modification. This was investigated in a few cases, for instance by using salts,[19] DNA intercalator,[20] supported lipid bilayer[21,22] and crowding effect with poly-(ethylene glycol).[23] Electrostatic interaction is a key-parameter[24] that has also been applied for formation of superlattice and new structures by addition of charged objects[25,26] as well as for actuation by simply applying voltage.[27] Here we report the discovery that 2D DNA origamis undergo a rapid and remarkable higher-order folding into self-folded 3D nanostructures, referred to as supra-folding, when they adsorb on cationic substrates prepared by layer-by-layer polyelectrolyte deposition. This supra-folding was found to be reversible, as the structures were efficiently unfolded back into their native 2D shapes upon addition of a competitive anionic polyelectrolyte. We investigated the role of the substrate in this phenomenon as well as the applicability of this actuation method to structurally reconfigure various DNA nanostructures including origamis of different shapes and functions as well as DNA nanogrids.

Figure 1 depicts our experimental system and demonstrates the main phenomenological results. Positively charged layers were created on negatively charged mica plates either by single layer adsorption of a cationic polyelectrolyte, or by sequential layer-by-layer (LbL) adsorption[28] of cationic and anionic polyelectrolytes (Figure 1 A). These polyelectrolyte-coated surfaces were then put in contact with a solution of tall-rectangle DNA origamis, prior to rinsing by buffer and direct imaging by atomic force microscopy (AFM) in liquid. Figures 1 B and C show AFM images of DNA origamis adsorbed on a monolayer of poly-L-Lysine (PLL) (M_w = 1000–5000 g mol^{-1}) and on a multilayer consisting of one layer of anionic polyelectrolyte (first arbitrarily chosen to be tall-rectangle origami staples) between two monolayers of PLL (PLL-staples-PLL), respectively. DNA origamis adsorbed on the PLL monolayer maintained their original shapes (Figure 1 B), as is usually observed for DNA origami adsorption on mica substrate either via ions present in the bulk (such as Mg^{2+} [29]) or previously treated by small multivalent cations (such as spermine[30]). In contrast, most of the tall-rectangle origamis adsorbed on the LbL multilayer appeared supra-folded into mainly rod-like shapes with one-third the area of the original origami and around 3 times its original height (Figure 1 C).

Other types of objects originating from tall-rectangle origamis were also observed on the LbL multilayers, which led us to categorize the adsorbed nanostructures into not supra-folded (UF: unfolded tall rectangles), three types of supra-foldamers (PF: partially supra-folded; 1SF: one-time supra-folded; 2SF: twice supra-folded), or aggregates of supra-folded structures (AG) (Figure 2 A, left). The unfolded state, which constituted the majority (87 %) of structures detected on monolayers, could not be detected anymore on multilayers where all objects were efficiently supra-folded and/or aggregated (Figure 2 B). Although the number of adsorbed objects increased with the adsorption time (t_{ads}), their distribution remained unchanged for $t_{ads} \geq 1$ min (Supporting Information, Figure S1), indicating that 1) the supra-folding of DNA origamis occurred during or right after their

[*] Dr. K. Nakazawa, F. El Fakih, Dr. V. Jallet, Dr. C. Rossi-Gendron, M. Mariconti, L. Chocron, Dr. M. Morel, Dr. S. Rudiuk, Prof. Dr. D. Baigl
PASTEUR, Department of Chemistry, Ecole Normale Supérieure PSL University, Sorbonne Université, CNRS
75005 Paris (France)
E-mail: sergii.rudiuk@ens.psl.eu
damien.baigl@ens.psl.eu
Dr. K. Nakazawa, Dr. M. Hishida, Prof. K. Saito
Department of Chemistry, University of Tsukuba
Tsukuba, Ibaraki 305-8571 (Japan)
Supporting information and the ORCID identification number(s) for the author(s) of this article can be found under: https://doi.org/10.1002/anie.202101909.

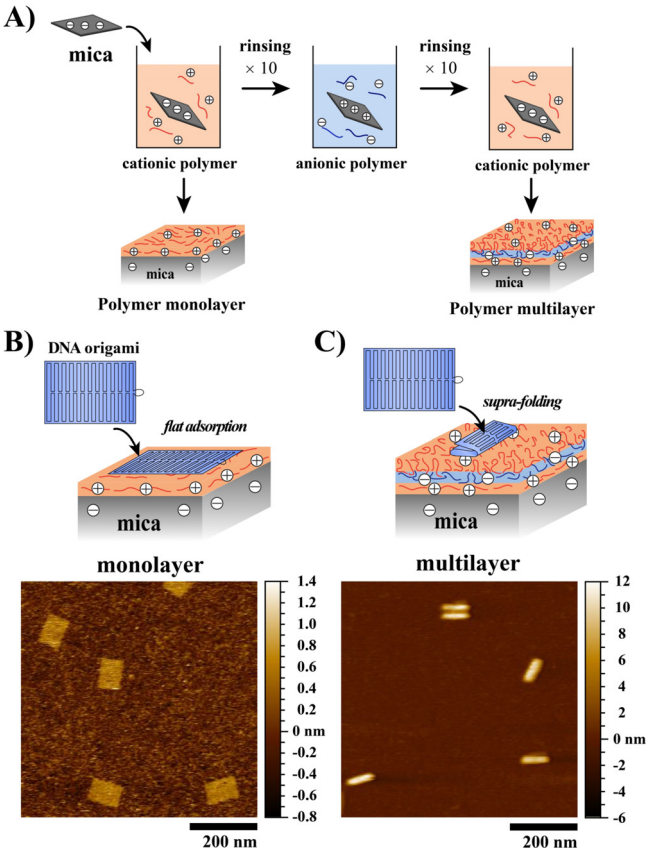

Figure 1. Illustration of our experiment and main results. A) We used as a substrate a mica plate coated by either a polycationic monolayer (left) or a multilayered structure prepared by the layer-by-layer (LbL) assembly of an anionic polyelectrolyte layer sandwiched between two cationic polyelectrolyte monolayers (right). Surfaces were thoroughly rinsed after each polyelectrolyte adsorption step and before origami adsorption. B),C) Atomic force microscopy (AFM) images in liquid of tall-rectangle DNA origamis adsorbed on a cationic monolayer (B) or on a LbL multilayer with poly-L-lysine (PLL, M_W = 1000–5000) as the cationic polymer and tall-rectangle staples as the anionic polymer (C).

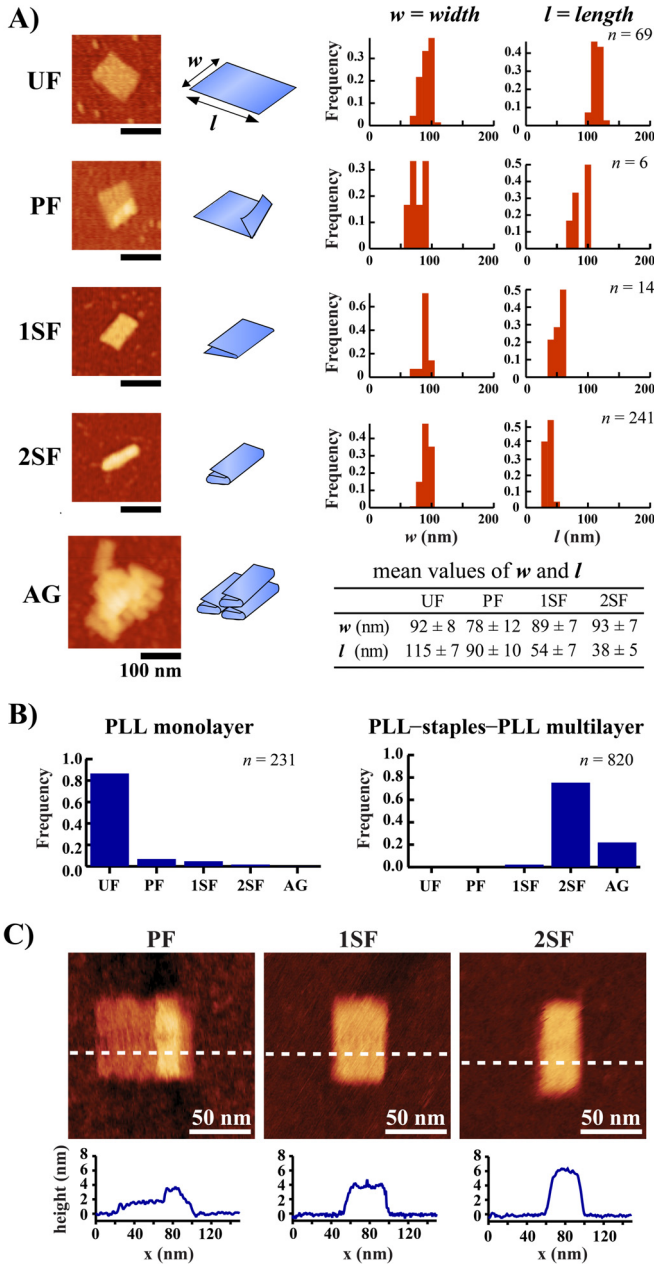

Figure 2. Categorization of the different objects observed after adsorption of tall-rectangle origamis. A) Representative AFM images (in air) and indicative illustrations of the different types of adsorbed objects (left); Frequency of characteristic dimensions parallel (*"width" w*) and perpendicular (*"length" l*) to the DNA double-helix direction of each of these objects (right); Values (mean ± sd) of *w* and *l* for each category (right bottom). The category name refers to the degree of supra-folding: no (UF), partial (PF), one-time (1SF) or twice (2SF). AG denotes aggregates of supra-folded structures. B) Relative frequency of each category observed on a PLL monolayer (left) and a PLL-staples-PLL multilayer (right). C) High-resolution AFM images in liquid (top) and height profile analysis (bottom) of individual PF (left), 1SF (middle) and 2SF (right) supra-foldamers. In all figures, *n* gives the total number of analyzed adsorbed DNA origamis.

adsorption on the multi-layered cationic surfaces and 2) it is a much faster process than conventional 3D origami assembly based on DNA base pairing.[8] Interestingly, the dimension parallel to the main double-helix direction in the initial tall rectangles (*"width" w*) stayed almost unchanged, whereas the perpendicular one (*"length" l*) underwent two- or three-fold decrease upon single or double supra-folding, respectively (Figure 2 A, right). These results show that supra-folding occurred parallel to the direction of double-stranded chains constructing the origamis, thus minimizing the bending of the DNA helices, a characteristic that was previously observed in programmed rolling behavior.[15] The supra-folding of tall-rectangle origamis was also accompanied by an increase of height from around 2 nm to 4 nm to 6 nm upon one-time and twice supra-folding, respectively (Figure 2 C), showing that origamis supra-folded on themselves while maintaining their internal self-assembled structure.

To understand the role of the substrate properties on the supra-folding behavior, we systematically investigated DNA origami adsorption on various monolayer- or multilayer-treated mica surfaces prepared as in Figure 1 and Figure 2 but with different kinds of cationic and anionic entities (Supporting Information, Figures S2,S4, Tables S1, S2). The polymeric

nature of the layers was found to be determinant as using spermine, a short tetraamine, resulted in a large majority of DNA origamis adsorbing flatly without supra-folding in both monolayered (99%) and multilayered (97%) substrates. In contrast, with cationic polyelectrolyte layers, the supra-folding yield was higher than with spermine, especially for long polyelectrolyte chains. This shows that polymeric connectivity between charges and conformational entropy in the adsorbed state (presence of loops), provided the substrate with more reconfigurability to electrostatically interact in 3D with the adsorbed origamis. Yet the supra-folding yield remained low with polymeric monolayers (Supporting Information, Figure S4, Table S2), probably because of their strong adsorption on the negatively charged mica substrate, leading to a high and rather flat cationic coverage (Figure 1B). Interestingly, supra-folding was systematically and dramatically enhanced in the case of polyelectrolyte multilayers (Supporting Information, Figure S2, Table S1). It is known that LbL multilayer deposition leads to loopy, interpenetrated layers forming a so-called "fuzzy" nanostructure.[28] The resulting substrates thus appeared to be ideally soft and reconfigurable to interact with origamis in 3D and induce their supra-folding (Figure 1C). Hence efficient supra-folding was observed with many kinds of LbL. This included 3-layered structures with a variety of cationic polyelectrolytes having different chemical natures (PLL, polyethylenimine), chain lengths and internal structures (linear and branched), as well as 5-layered structures (PLL-staples-PLL-staples-PLL; Supporting Information, Figure S5). When we changed the intermediate anionic layer to sodium polystyrenesulfonate, supra-folding efficiency was low, a peculiar behavior that might be due to a flatter conformation in the adsorbed state leading to a less loopy cationic surface. However, for all other tested anionic polyelectrolytes, such as double-stranded DNA of different sequences (salmon sperm DNA and lambda-phage DNA), efficient supra-folding was obtained (Supporting Information, Figure S3, Table S1), excluding a specific role of sequences and lengths of the nucleic acids used as intermediate layers. All these results demonstrate that supra-folding occurred upon origami adsorption when the substrate combined cationic surface charge with enough fuzziness to provide tridimensional reconfigurability and charge accessibility.

Since the supra-folding mechanism shared analogy with inter-polylectrolyte complexation,[31] we explored the possibility of unfolding the supra-foldamers by adding a polyanion competitor, heparin, known to efficiently unfold electrostatically complexed linear DNA.[32,33] To this end, DNA origamis were first adsorbed on the PLL-staples-PLL multilayer, and we observed in situ their evolution over time by live AFM imaging in liquid at a fixed position (Figure 3; Supporting Information, Movies S1,S2). The majority of origamis were found to be supra-folded on the substrate and did not evolve as long as the outer medium composition remained constant. In contrast, as soon as heparin was added to the medium, we observed a rapid evolution of the adsorbed supra-foldamers. In a few minutes, the height of each individual object decreased, accompanied by a planar extension perpendicular to the supra-folding direction. After 20 minutes of exposure, most of DNA structures adopted a stable shape reproducing the geometric features of the origami rectangles before their supra-folding. Successful unfolding was also observed by heparin addition to origamis initially surpa-folded on a LbL composed of 5 layers (Supporting Information, Figure S5). Addition of heparin thus induced in situ unfolding of adsorbed supra-foldamers back to their original 2D shape and confirmed the interpolyelectrolyte complexation nature of the supra-folding mechanism.

Finally, we assessed the robustness of our actuation method for the structural 2D/3D reconfiguration of DNA assemblies with various structures, shapes, and functionality (Figure 4; Supporting Information, Figure S6). First, similarly to tall rectangles, origamis with other shapes, such as smiley- and triangle-shaped origamis, adsorbed flatly on the cationic monolayer but adopted supra-folded structures when adsorbed on the LbL multilayer and successfully unfolded back to their initial states upon exposure to heparin (Supporting Information, Figure S7). Fine structural details, even in complex shapes such as smileys were well preserved as shown by the identical mean eye-to-eye distance before ($d = 32.0 \pm 1.3$ nm, $n = 252$) and after a sequence of supra-folding and heparin-induced unfolding ($d = 32.3 \pm 1.2$ nm, $n = 116$; Figure 4A; Supporting Information, Table S3).

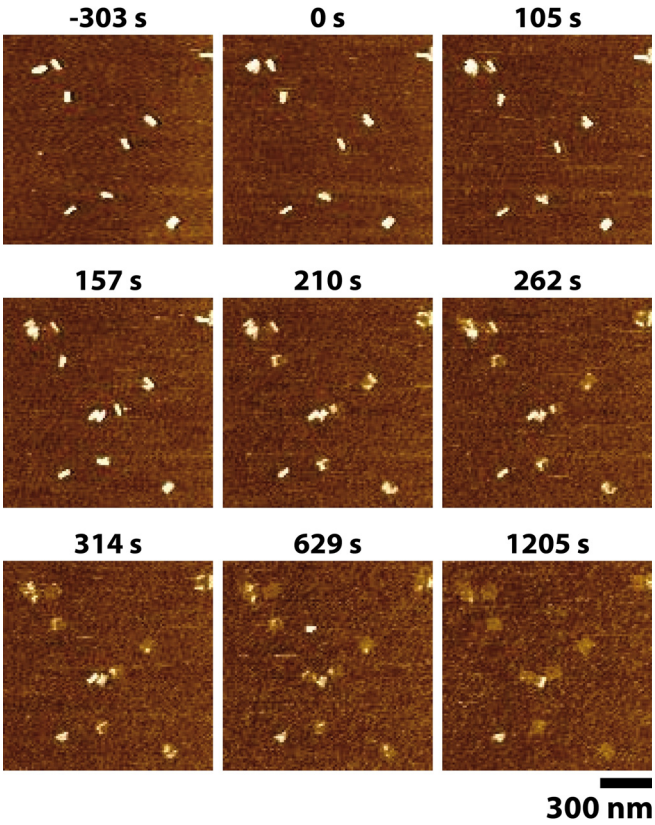

Figure 3. Heparin-induced unfolding of adsorbed origami supra-foldamers followed by live AFM imaging in liquid. Rectangle origamis adsorbed on a PLL-staples-PLL multilayer were imaged continuously using AFM in liquid. Heparin (9 μM in sulphate and carboxylate groups) was added at $t = 0$. Images are extracted from Movie S1 (Supporting Information).

Similarly, protein-tethered origamis (Figure 4B left image) adsorbed flatly on the PLL monolayer but supra-folded into 3D structures on the LbL substrate with a dramatic modification of the spatial protein distribution (Figure 4B middle image, where detected proteins are pointed by arrowheads). Remarkably, heparin treatment led to unfolding of the protein-functionalized origamis into their initial state (Figure 4B right image), with a perfect recovery of the characteristic protein-protein distances (Figure 4B distributions and Supporting Information, Table S3). The same supra-folding → unfolding sequence was applied to biotinylated triangle-shaped origamis (Figure 4C). Notably, further addition of streptavidin led to successful origami functionalization by the proteins (Figure 4C right image) at the same positions (Figure 4C distributions and Supporting Information, Table S3) as in identical origamis but functionalized before supra-folding (Figure 4B; Supporting Information, Table S3). This shows that not only structural features but also functionality (here biotin reactivity) were preserved upon supra-folding and successive unfolding. The size of DNA origamis we studied was limited by the necessity of using a finite-size scaffold. To know whether 3D structures of higher dimension could be obtained, we characterized the supra-folding behavior of so-called DNA nanogrids, which are scaffold-free and extended self-assembled structures composed by the repetition of a square motif of complementary oligonucleotides.[34] The motif size of the used nanogrid was 17 nm (Figures 4D left, 4E). Remarkably, upon adsorption on the LbL multilayer, the nanogrids spontaneously supra-folded into well-defined 3D ribbons (Figure 4D, right) with a width of around 75 nm, a length of a few micrometers (Figure 4F) and a height between twice and three times larger than that of the initial 2D grid (Figure 4G). The initial grid structure was preserved in the resulting ribbons, with a similar periodicity and square motif size (Figure 4G). All these results show that supra-folding is a versatile method for the fast supra-folding of 2D DNA assemblies into 3D nanostructures that range from a compact size (DNA origami) to extended dimensions

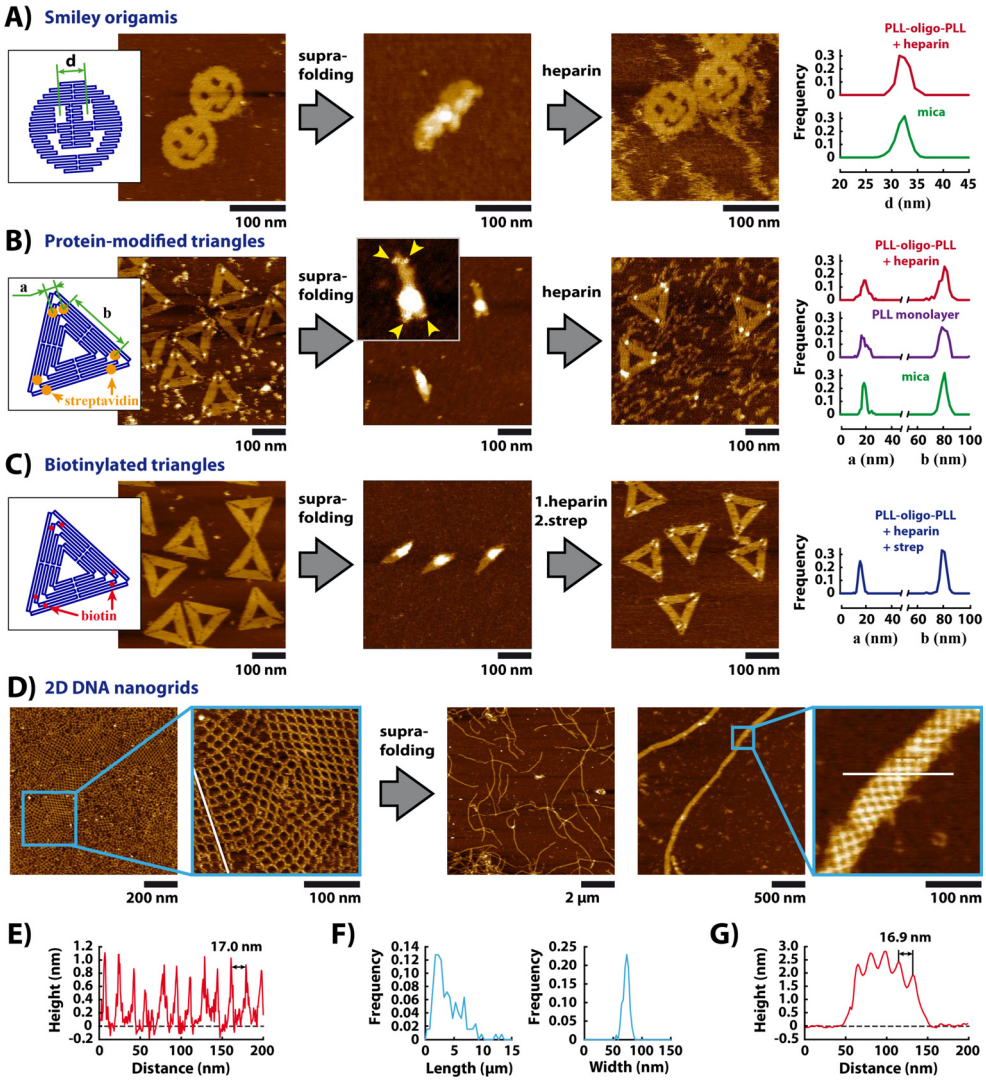

Figure 4. Supra-folding versatility demonstrated with various DNA nanostructures adsorbed on a PLL-staples-PLL multilayer. A)–C) Smiley-shaped origamis (A), streptavidin-functionalized triangle-shaped origamis (B) and biotinylated triangle-shaped origamis (C) as observed by AFM in liquid before supra-folding (left, on mica), and after supra-folding on the multilayer before (middle) and after (right) addition of 15 µM heparin (A,B) or successive addition of 15 µM heparin and 2 µM streptavidin (C). Arrowheads in (B) indicate proteins in the supra-folded state. Graphics on the right display the distribution of characteristic lengths measured on a large number (*n*) of origamis: A) distance *d* between the smiley "eye" centers on mica (green) or after supra-folding and unfolding by heparin (red); B) distances between two tethered proteins in the same corner (*a*) or in the same edge (*b*) of origamis adsorbed on mica (green), on a PLL monolayer (purple) or on the PLL-staples-PLL multilayer after a sequence of supra-folding and heparin-induced unfolding (red); C) distances between tethered proteins (as defined in B) after supra-folding biotinylated triangles, unfolding by heparin and addition of streptavidin. D) AFM images in liquid of 2D DNA nanogrids before (left panels, on mica) and after supra-folding on the multilayer (right panels). E) Height profile in a nanogrid along the white line shown in D (second panel from the left). F) Size distribution of the length and width of the supra-folded ribbons observed in D. G) Height profile in a supra-folded ribbon along the white line shown in D (last panel on the right).

(nanogrids) and preserve both DNA structural features and site-specific functionality.

In summary, the present study revealed that 2D DNA nanostructures could undergo efficient and fast supra-folding on positive layer-by-layer polyelectrolyte substrates to give 3D supra-foldamers of nanometric (supra-folded origamis) to micrometric (ribbons) dimensions. Orthogonal to DNA base-pairing, this actuation mechanism was proven efficient on various systems including DNA origamis of different shapes and functionality and DNA nanogrids, thus carrying a general character potentially applicable to many kinds of DNA-based nanostructures. Interestingly, this actuation principle was shown to be reversible as addition of heparin resulted in efficient switching of the supra-folded origamis back to their original 2D shape, in which structural features, reactivity and site-specific functionality were well preserved. Limited here to DNA-scaffolded streptavidin assemblies, we expect it to be applicable to the dynamically addressable DNA-scaffolding of various types of guests including functional proteins, active peptides, chemical groups or colloids. These results thus further emphasize some of the unique properties of fuzzy nano-assemblies produced by LbL as well as propose a simple yet novel and robust principle for the generic and reversible actuation of 2D/3D DNA-based nanostructures.

Acknowledgements

We thank M. Yokokawa (University of Tsukuba) for experimental support. This work was supported by the European Research Council (ERC) (European Community's Seventh Framework Programme (FP7/2007–2013)/ERC Grant Agreement No. 258782, D.B.), the French National Research Agency ANR contracts DYOR (ANR-18-CE06-0019, D.B.) and ActiveGEL (ANR-18-CE07-0001, S.R.), a Grant-in-Aid for JSPS Research Fellows (grant no. 15J04751, K.N.), and a JSPS Overseas Research Fellowships (K.N).

Conflict of interest

The authors declare no conflict of interest.

Keywords: actuation · DNA nanogrids · DNA nanotechnology · DNA origami · layer-by-layer

[1] J. D. Watson, F. H. C. Crick, *Nature* **1953**, *171*, 737 – 738.
[2] L. Adleman, *Science* **1994**, *266*, 1021 – 1024.
[3] M. R. Jones, N. C. Seeman, C. A. Mirkin, *Science* **2015**, *347*, 1260901.
[4] W. B. Rogers, W. M. Shih, V. N. Manoharan, *Nat. Rev. Mater.* **2016**, *1*, 16008.
[5] F. Hong, F. Zhang, Y. Liu, H. Yan, *Chem. Rev.* **2017**, *117*, 12584 – 12640.
[6] P. W. K. Rothemund, *Nature* **2006**, *440*, 297 – 302.
[7] S. M. Douglas, A. H. Marblestone, S. Teerapittayanon, A. Vazquez, G. M. Church, W. M. Shih, *Nucleic Acids Res.* **2009**, *37*, 5001 – 5006.
[8] S. M. Douglas, H. Dietz, T. Liedl, B. Högberg, F. Graf, W. M. Shih, *Nature* **2009**, *459*, 414 – 418.
[9] D. Han, S. Pal, J. Nangreave, Z. Deng, Y. Liu, H. Yan, *Science* **2011**, *332*, 342 – 346.
[10] H. Jun, F. Zhang, T. Shepherd, S. Ratanalert, X. Qi, H. Yan, M. Bathe, *Sci. Adv.* **2019**, *5*, eaav0655.
[11] B. Saccà, C. M. Niemeyer, *Angew. Chem. Int. Ed.* **2012**, *51*, 58 – 66; *Angew. Chem.* **2012**, *124*, 60 – 69.
[12] E. S. Andersen, M. Dong, M. M. Nielsen, K. Jahn, R. Subramani, W. Mamdouh, M. M. Golas, B. Sander, H. Stark, C. L. P. Oliveira, et al., *Nature* **2009**, *459*, 73 – 76.
[13] E. Benson, A. Mohammed, J. Gardell, S. Masich, E. Czeizler, P. Orponen, B. Högberg, *Nature* **2015**, *523*, 441 – 444.
[14] Y. Ke, L. L. Ong, W. M. Shih, P. Yin, *Science* **2012**, *338*, 1177 – 1183.
[15] H. Chen, T. W. Weng, M. M. Riccitelli, Y. Cui, J. Irudayaraj, J. H. Choi, *J. Am. Chem. Soc.* **2014**, *136*, 6995 – 7005.
[16] H. Ijäs, S. Nummelin, B. Shen, M. Kostiainen, V. Linko, *Int. J. Mol. Sci.* **2018**, *19*, 2114.
[17] J. K. Daljit Singh, M. T. Luu, A. Abbas, S. F. J. Wickham, *Biophys. Rev.* **2018**, *10*, 1283 – 1293.
[18] B. Yurke, A. J. Turberfield, A. P. Mills, F. C. Simmel, J. L. Neumann, *Nature* **2000**, *406*, 605 – 608.
[19] C. Kielar, S. Ramakrishnan, S. Fricke, G. Grundmeier, A. Keller, *ACS Appl. Mater. Interfaces* **2018**, *10*, 44844 – 44853.
[20] H. Chen, H. Zhang, J. Pan, T. G. Cha, S. Li, J. Andréasson, J. H. Choi, *ACS Nano* **2016**, *10*, 4989 – 4996.
[21] Y. Sato, M. Endo, M. Morita, M. Takinoue, H. Sugiyama, S. Murata, S. M. Nomura, Y. Suzuki, *Adv. Mater. Interfaces* **2018**, *5*, 1800437.
[22] Y. Suzuki, M. Endo, H. Sugiyama, *Nat. Commun.* **2015**, *6*, 8052.
[23] M. W. Hudoba, Y. Luo, A. Zacharias, M. G. Poirier, C. E. Castro, *ACS Nano* **2017**, *11*, 6566 – 6573.
[24] S. Møller Sønderskov, L. Hyldgaard Klausen, S. Amland Skaanvik, X. Han, M. Dong, *ChemPhysChem* **2020**, *21*, 1474 – 1482.
[25] S. Julin, A. Korpi, Nonappa, B. Shen, V. Liljeström, O. Ikkala, A. Keller, V. Linko, M. A. Kostiainen, *Nanoscale* **2019**, *11*, 4546 – 4551.
[26] J. Mikkilä, A. P. Eskelinen, E. H. Niemelä, V. Linko, M. J. Frilander, P. Törmä, M. A. Kostiainen, *Nano Lett.* **2014**, *14*, 2196 – 2200.
[27] E. Kopperger, J. List, S. Madhira, F. Rothfischer, D. C. Lamb, F. C. Simmel, *Science* **2018**, *359*, 296 – 301.
[28] G. Decher, *Science* **1997**, *277*, 1232 – 1237.
[29] D. Pastré, O. Piétrement, S. Fusil, F. Landousy, J. Jeusset, M. O. David, L. Hamon, E. Le Cam, A. Zozime, *Biophys. J.* **2003**, *85*, 2507 – 2518.
[30] M. Tanigawa, T. Okada, *Anal. Chim. Acta* **1998**, *365*, 19 – 25.
[31] A. Estévez-Torres, D. Baigl, *Soft Matter* **2011**, *7*, 6746 – 6756.
[32] E. Ramsay, J. Hadgraft, J. Birchall, M. Gumbleton, *Int. J. Pharm.* **2000**, *210*, 97 – 107.
[33] S. Rudiuk, S. Franceschi-Messant, N. Chouini-Lalanne, E. Perez, I. Rico-Lattes, *Langmuir* **2008**, *24*, 8452 – 8457.
[34] H. Yan, S. H. Park, G. Finkelstein, J. H. Reif, T. H. LaBean, *Science* **2003**, *301*, 1882 – 1884.

Manuscript received: February 6, 2021
Accepted manuscript online: March 6, 2021
Version of record online: April 14, 2021

